European Review for Medical and Pharmacological Sciences 2020; 24: 6540-6550

Circ100284 promotes invasion and migration of osteosarcoma cells by down-regulating PTEN and EMP1

Y.-D. LIU[1], L.-P. LIU[2]

[1]Department of Osteoarthrosurgery, Jining No. 1 People's Hospital, Jining, China
[2]Department of Oncology, Jining No. 1 People's Hospital, Jining, China

Abstract. – OBJECTIVE: To investigate the role of circ100284 in osteosarcoma (OS) and the underlying mechanism.

PATIENTS AND METHODS: Quantitative Real Time-Polymerase Chain Reaction (qRT-PCR) was used to detect the level of circ100284 in OS tissues and cells, and to examine the association between its level and clinicopathological features such as tumor size, tumor stage, and survival time. In addition, circ100284 was knocked out in MG63 and U2OS cells to observe the effect of circ100284 on cell viability, migration, cycle, and apoptosis by Cell Counting Kit-8 (CCK-8), transwell assay, and flow cytometry assay. Correlations of circ100284 with lysine-specific histone demethylase 1A (LSD1) and enhancer of zeste homolog 2 (EZH2) target proteins were analyzed by RNA co-precipitation experiments. Furthermore, the chromatin immunoprecipitation assay (ChIP)-qPCR assay was performed to analyze the relationship between circ100284 and its target protein and target gene.

RESULTS: Circ100284 had a high level in OS tissues. The high expression of circ100284 was positively correlated with tumor size, pathological stage, and lung metastasis, and negatively correlated with patient survival time. Knocking down circ100284 in OS cells damaged the cell viability and invasiveness, blocked cell cycle, and promoted cell apoptosis. Further experiments showed that circ100284 could epigenetically inhibit cell proliferation by negatively regulating Phosphatase and tensin homolog (PTEN) and epithelial membrane protein 1 (EMP1) in OS.

CONCLUSIONS: Circ100284 promotes the progression of OS cells by downregulating PTEN and EMP1.

Key Words:
Circ100284, PTEN, EMP1, Osteosarcoma.

Introduction

Osteosarcoma (OS) is the most common primary malignant bone tumor[1]. It mostly occurs in children and adolescents aged 10-20 years old[2]. Its complex pathogenesis and resistance to conventional treatment lead to high mortality and poor prognosis. After neoadjuvant chemotherapy and surgery, the 5-year survival rate of patients could increase to 60%-80%[3]. However, due to the high degree of malignancy, early metastasis, and resistance to chemotherapy drugs, OS still has the risk of local recurrence or distant metastasis[4]. Therefore, new therapeutic strategies and innovative therapies are urgently needed to further prolong the survival of patients with OS. Many scholars have begun to use the etiology and molecular biology research to achieve the goal of clinically curing OS, of which the key is to improve the drug resistance of OS.

Circular RNAs (circRNAs) are newly discovered non-coding RNAs (ncRNAs) containing a special covalently closed circular structure with neither 5'-3' polarity nor polyadenylation tail[5]. In 1970s, circRNA was discovered in RNA viruses[6], but in the past 30 years, only a small number of circRNAs have been confirmed[7-13]. Most circRNAs are exonic circRNAs (ecircRNAs), which are mainly found in the cytoplasm. The circRNA molecule is rich in miRNA response elements (MRE)[14-16], which can adsorb specific miRNAs through these MREs and act as molecular "sponges" of miRNAs, thereby regulating the function of miRNAs[16,17]. Some circRNAs are encoded by circular intronic RNA (ciRNA), or exon and intron circRNAs (EIciRNAs), which are located in the nucleus and are involved in the regulation of gene transcription[18,19].

In recent years, many studies have confirmed that circRNA is associated with the development of tumors. Li et al[20] found that cir-ITCH was downregulated in esophageal squamous cell carcinoma. Cir-ITCH can upregulate ITCH by adsorbing miR-7, miR-17, and miR-124, thereby suppressing esophageal squamous cells by inhibiting the Wnt signaling pathway. Moreover, Bachmayr-Heyda

Corresponding Author: Liping Liu, BM; e-mail: dr_liuliping@163.com

et al[21] found that circRNA expression was widely downregulated in colorectal cancer, and the abundance of circRNA expression was negatively correlated with cell proliferation. Circ100284 is a newly discovered circular RNA, and there are few studies on its relationship with OS. Xue et al[22] found that circ100284 can regulate enhancer of zeste homolog 2 (EZH2) through miR-217. Dai et al[23] found that circ100284 is involved in arsenite-induced malignant transformation of hepatic epithelial (L-02) cells. However, the role of circ100284 in OS has not been reported so far.

Therefore, in this study, the role of circ100284 in OS tissues and cells and its underlying mechanism were explored.

Patients and Methods

Clinical Sample Collection

A total of 52 human OS tissue samples and adjacent normal tissue samples were collected from patients and quickly frozen in liquid nitrogen at -80°C for the following experiments. Their clinical data, including age, gender, tumor size, tumor stage, and presence of lung metastases, were collected. All of the above tissue products were collected under the consent of the patients and the approval of the Ethics Committee of Jining No. 1 People's Hospital.

Cell Culture and Transfection

Human OS cell lines MG-63, U2OS, and SAOS-2 and a normal osteoblast cell line (Hfob 1.19) were purchased from the Shanghai Institute of Cell Biology, Chinese Academy of Sciences (Shanghai, China). The cells were cultured in a cell culture incubator at 37°C, 5% CO_2 with Roswell Park Memorial Institute-1640 (RPMI-1640) medium (HyClone, South Logan, UT, USA) containing 100 mL/L fetal bovine serum (FBS; Gibco, Rockville, MD, USA), 100 IU/mL penicillin, 100 μg/mL streptomycin. When cell density reached 90%, the cells were passaged to maintain the logarithmic growth state. Si-circ100284 1#, si-circ100284 2# were purchased from GenePharma (Shanghai, China), and transfection experiment was performed using Lipofectamine 2000 Reagent (Invitrogen, Carlsbad, CA, USA).

Cell Counting Kit-8 (CCK-8)

The cells were seeded in a 96-well plate at 5000 cells per well with 5 replicate wells. Cell viability at 6, 24, 48, 72, and 96 h were detected, respectively by CCK-8 assay (Dojindo, Kumamoto, Japan). Then, the optical density (OD) value of each well at 450 nm was measured by a TECAN infinite M200 Multimode plate reader.

Quantitative Real Time-Polymerase Chain Reaction (qRT-PCR)

RNAs were extracted using the TRIzol reagent (Invitrogen, Carlsbad, CA, USA) and reversely transcribed into complementary deoxyribose nucleic acids (cDNAs). QPCR was performed using SYBR Green I fluorescence method, and the relative gene expression was analyzed based on $2^{-\Delta\Delta CT}$ method. The reaction system volume was in total 25 μl, pre-denaturation at 95°C for 5 min, denaturation at 95°C for 30 sec, annealing at 60°C for 45 sec, extension at 72°C for 3 min, with 35 cycles, and then, extension at 72°C for 5 min. Quantitative analysis was carried out using the ABI 7500 fluorescence PCR amplification instrument (Applied Biosystems; Foster City, CA, USA). Circ100284 primer sequences: F: 5'-ACTCACAATGATCCAAAAGGAGT-3', R: 5'-GAGATACAGTGCATTCCAAGACA-3'. GAPDH: F: 5'-TGACTTCAACAGCGACACCCA-3', R: 5'-GGAGTGTTGGAGAAGTCATATTAC-3'.

Transwell Assay

Transfected MG-63 and U2OS cells (1×10^5) were added to the upper chamber pre-coated with Matrigel in serum-free medium. At the same time, 500 μL of Dulbecco's Modified Eagle's Medium (DMEM) (Gibco, Rockville, MD, USA) containing 10% FBS was added in the lower chamber. After 48 h of incubation, the cells remaining on the upper chamber were scraped off. Finally, the cells migrating or invading the membrane in each group were fixed with methanol, stained with crystal violet, imaged, and counted.

Western Blotting

The transfected cells were collected and lysed by an appropriate amount of cell lysate to obtain total cell protein solution. Each protein sample was subjected to sodium dodecyl sulphate-polyacrylamide gel electrophoresis (SDS-PAGE) and transferred to a polyvinylidene difluoride (PVDF) membrane (Millipore, Billerica, MA, USA). After transfection, the cells were blocked with blocking solution for 1 h, and then, incubated at 4°C with the primary antibodies for one night. After washed in Tris-Buffered Saline-Tween (TBST) for 3 times, the membrane was incubated with secondary antibody (goat anti-rabbit) for 2 h at

room temperature, and then, washed with TBST for 3 times with 10 min each time. The protein bands were determined by imaging analysis system and enhanced chemiluminescence (ECL) imaging (Gel-ProAnalyzer software, United Bio, Wichita, KS, USA).

Cell Cycle Detection

MG63 and U2OS cells were transfected with si-NC and si-circ100284, respectively. After 24 h, the cells were fixed with 75% ethanol overnight at 4°C. After treatment with RNase A at 37°C for 30 minutes and stained with propidium iodide, the cell cycle was detected by examining 10^5 nuclei using a FACS Calibur flow cytometer (Becton Dickinson, Franklin Lakes, NJ, USA).

Cell Apoptosis Detection

The cells were transfected with si-NC and si-circ100284. After 24-48 h, cells were trypsinized into cell suspension, and then, separated and placed into the corresponding flow tube. After washed 2 times with pre-cooled phosphate-buffered saline (PBS), the cells were then added with 200 μL of binding buffer containing calcium ions and 10 μL of Annexin V-FITC (fluorescein isothiocyanate) fluorescent probe. After incubation on ice for 15 min in the dark, 5 μL of propidium iodide (PI) was added into the cell solution for incubation on ice for 5 min. Cell apoptosis was detected using the FL1 and FL3 dual-channel wavelength by the flow cytometer (FACSCalibur; BD Biosciences, Detroit, MI, USA).

Chromatin Immunoprecipitation Assay (ChIP)

The cells (1×10^7) were incubated for 24 h and cross-linked in 1% formaldehyde for 10 min. After cell lysis, chromatin was fragmented to an average size of 500 bp. The antibody was conjugated with Dynal beads (Invitrogen, Carlsbad, CA, USA), and incubated with anti-EZH2 and H3K27me3 or homotypic IgG at 4°C overnight. The cross-linking of the enriched and input DNA was then reversed, and the DNA was washed with RNase A (0.2 mg/mL) and proteinase K (2 mg/mL) prior to phenol/chloroform purification. The sequence of the immunoprecipitated and input DNA was determined by PCR primers.

RNA Binding Protein Immunoprecipitation (RIP) Assay

A complete RIP lysis buffer (Abcam, Cambridge, MA, USA) was prepared and placed on ice. When the confluence of the monolayer adherent cells reached 80%-90%, the cells were washed with pre-cooled PBS (10 mL, twice), scraped with a cell scraper and transferred to a 15 mL sterile EP tube. After centrifugation at 4°C and 1500 g for 5 min, the supernatant was discarded, and then, cells were resuspended with complete RIP lysate. After made into aliquot of 200 μL, the lysate was stored in a -80°C refrigerator for further analysis.

Statistical Analysis

Data analysis was performed using Statistical Product and Service Solutions (SPSS) 20.0 (IBM Corp., Armonk, NY, USA) and GraphPad statistical software (La Jolla, CA, USA). The data were expressed as mean ± standard deviation ($\bar{x}\pm s$), and the *t*-test was used for comparison between two groups. For the analysis of three groups, the analysis of variance followed by the post-hoc test (Least Significant Difference) was applied. The relationship between the expression level of circ100284 and the clinical pathology of patients was tested by Chi-square test. $p<0.05$ was considered statistically significant.

Results

Circ100284 Was Highly Expressed in Osteosarcoma

To detect the role of circ100284 in OS, the level of circ100284 in OS patients was analyzed by qRT-PCR. The results showed that circ100284 was highly expressed in OS patients compared with that in adjacent tissues (Figure 1A). Then, the relationship between the expression of circ100284 and clinical pathological features in 52 patients with OS was further detected. Patients were divided into high circ100284 expression group and low circ100284 expression group according to the median expression of circ100284 in 52 patients with OS (Figure 1B). The results showed that circ100284 expression was associated with tumor size, WHO grade, and lung metastasis (Table I). As shown in Figure 1C, circ100284 expression showed a positive correlation with tumor stage, which was gradually increased with the increase of WHO grade stage (Figure 1C). A prognostic analysis of the patients found that the circ100284 high-expression group had a poorer survival rate than the circ100284 low-expression group (Figure 1D). The above results indicate that circ100284 is aberrantly highly expressed in OS and that circ100284 expression is correlated with the disease survival.

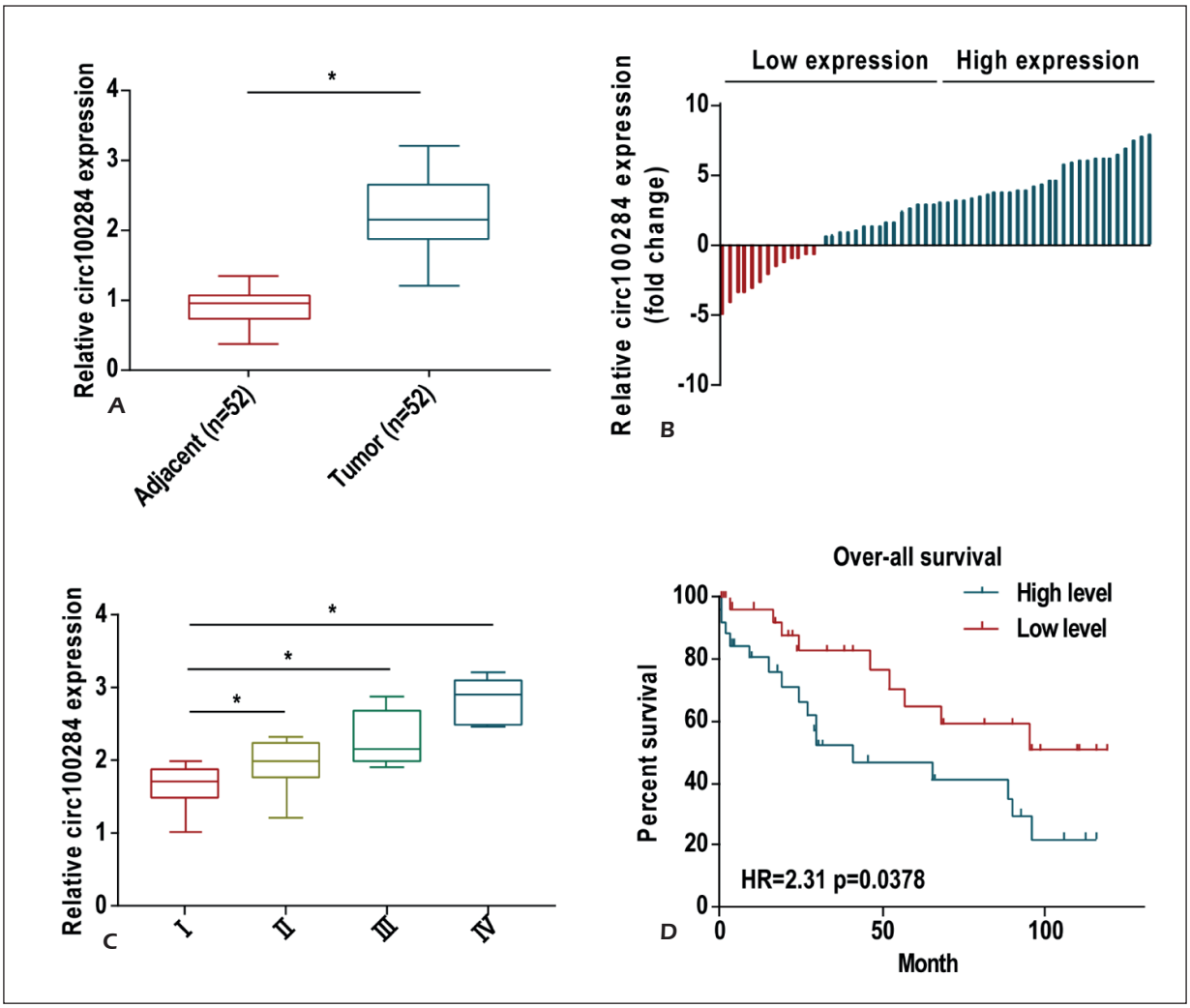

Figure 1. Circ100284 is highly expressed in OS. **A**, and **B**, qRT-PCR reveals that the expression of circ100284 in OS tumor tissues is significantly higher than that in adjacent tissues. **C**, qRT-PCR manifests that circ100284 is markedly higher in tumors of stage II, III, and IV patients than of stage I patients. **D**, The overall survival of OS patients with high expression of circ100284 is significantly lower than that of patients with low expression. *$p<0.05$.

Silencing Circ100284 Inhibited Proliferation of Osteosarcoma Cells

The expression levels of circ100284 in normal osteoblasts (Hfob 1.19) and OS cell lines (MG63, U2OS, HOS, and Saos2) were examined by qRT-PCR assay. It was found that circ100284 was significantly higher in OS cell line (MG63, the expression in U2OS, HOS, and Saos2) than that in the normal osteoblast line (Figure 2A). After further knocking down circ100284 in MG63 and U2OS cells, the silencing efficiency was detected by qRT-PCR (Figure 2B). The CCK8 assay results suggested that the cell viability was decreased after the knockdown of circ100284 (Figure 2C). Besides, transwell assay results demonstrated that cell migration and invasion were reduced after the knockdown of circ100284 (Figure 2D). Additionally, flow cytometry results confirmed that the silencing of circ100284 stopped the cell cycle in G0/G1 phase and increased the cell apoptosis (Figure 2E and 2F). These above results reveal that the inhibition of the expression of circ100284 can inhibit the proliferation of OS cells and promote cell apoptosis.

Circ100284 Could Regulate Phosphatase and Tensin Homolog (PTEN) and Epithelial Membrane Protein 1 (EMP1) in OS

To explore the specific mechanism of circ100284 in MG63 and U2OS cells, qRT-PCR was used to detect the mRNA expression levels of KLF2, PTEN, EMP1, CDKN1A, CDKN2B, and Bcl-2 after circ100284 silencing. The results

Table I. Correlation between expression of circ100284 and clinicopathological features in patients with osteosarcoma (n = 52).

Clinicopathologic features	Number of cases	circ100284 expression		*p*-value
		Low (n=26)	High (n=26)	
Age (years)				0.5745
≤20	30	16	14	
>20	22	10	12	
Gender				0.5780
Male	28	13	15	
Female	24	13	11	
Tumor size				0.0247*
≤6CM	30	16	8	
>6CM	22	10	18	
WHO grade				0.0125*
I-II	27	18	9	
III-IV	25	8	17	
Pulmonary metastasis				0.0110*
Yes	21	15	6	
No	31	11	20	

showed that the expressions of PTEN, EMP1, CDKN1A, and Bcl-2 mRNA were increased, while the expressions of KLF2 and CDKN2B were not significantly changed (Figure 3A). In MG63 cells, RNA co-immunoprecipitation assays were carried out to detect the binding of circ100284 to lysine-specific histone demethylase 1A (LSD1) and EZH2, which showed that circ100284 could directly bind to LSD1 and EZH2 (Figure 3B). In MG63 cells, after LSD1 and EZH2 were knocked down, qRT-PCR revealed significant decreases in the expressions of LSD1 and EZH2 (Figure 3C and 3D). The above results indicate that PTEN, EMP1, CDKN1A, and Bcl-2 can be regulated by circ100284.

Circ100284 Apparently Silencing PTEN and EMP1 by Combining with LSD1 and EZH2

To explore the mechanism of circ100284 on OS cells, LSD1, and EZH2 in MG63 cells were knocked down, and the mRNA expression levels of KLF2, PTEN, EMP1, CDKN1A, CDKN2B and Bcl-2 were detected by qRT-PCR. The results showed that the expressions of KLF2, PTEN, EMP1, CDKN2B and Bcl-2 mRNA were upregulated after knockdown of LSD1, while the expression of CDKN1A was not significantly changed (Figure 4A). After knocking down EZH2, the expressions of KLF2, PTEN, EMP1, CDKN1A, and CDKN2B were significantly upregulated (Figure 4B). Meanwhile, after knockdown of circ100284, LSD1, and EZH2, the results of the co-variation of the genes showed that only PTEM and EMP1 showed sustained upregulation (Figure 4C). Therefore, ChIP-qPCR assay was used to detect the binding of LSD1, H3K27me3, and EZH2 to the PTEN promoter region. The results showed that EZH2, H3K27me3, and LSD1 reduced binding to the PTEN and EMP1 promoter regions, while H3K4me2 increased binding to the PTEN and EMP1 promoter regions after circ100284 knockdown (Figure 4D and 4E). These above results indicated that circ100284 can inhibit the expressions of PTEN and EMP1 in OS by binding to LSD1 and EZH2.

Circ100284 Negatively Regulates the Expression of PTEN and EMP1

Furthermore, the expressions and roles of PTEN and EMP1 in OS tissues were also examined. QRT-PCR results revealed that PTEN and EMP1 expressions were significantly lower in OS tissues than in adjacent tissues (Figure 5A and 5B). After knockdown of PTEN and EMP1 in MG63 cells, qRT-PCR results displayed a significant decrease in the expressions of PTEN and EMP1 (Figure 5C and 5D). Further Western blotting analysis confirmed that the protein expression levels were decreased after knockdown of PTEN and EMP1 (Figure 5E). In addition, the CCK8 assay showed that after knocking down PTEN or EMP1, cell viability was enhanced (Figure 5F). In MG63 cells, the knockdown of circ100284 and knockdown of PTEN or EMP1 reversed the decrease in cell viability caused by simple knockdown of circ100284 (Figure 5G). Similarly, tran-

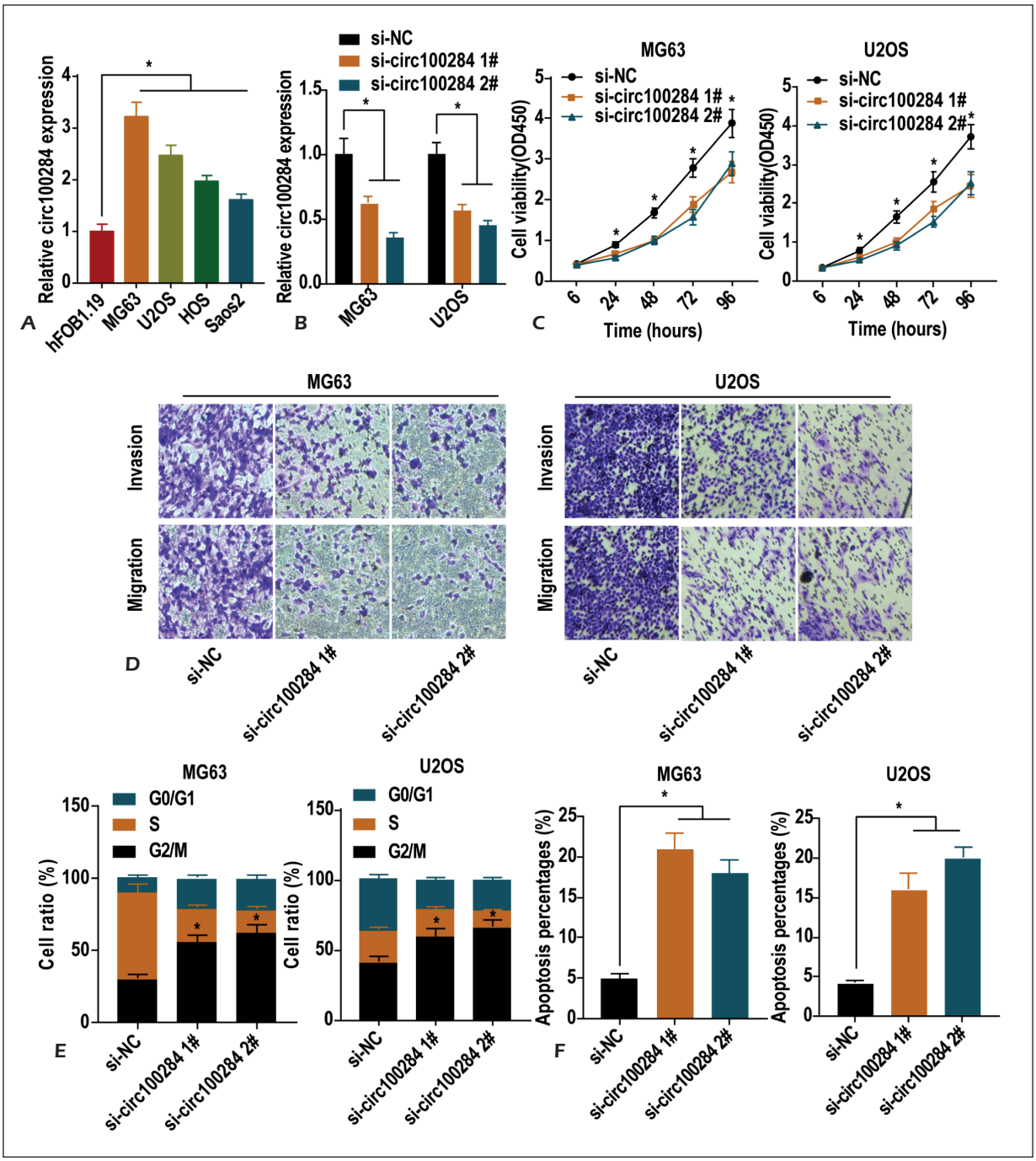

Figure 2. Silencing circ100284 can inhibit the proliferation of OS cells. **A**, qRT-PCR detection indicates that circ100284 expression in OS cells (MG63, U2OS, HOS, and Saos2) is significantly higher than that in normal osteoblast cell line (Hfob 1.19). **B**, After knocking down circ100284 in MG63 and U2OS cells, the expression of circ100284 is remarkably decreased. **C**, CCK8 reveals that cell viability is decreased. **D**, Transwell assay is used to detect the migration and invasion of cells (magnification: 40×). E, Flow cytometry reveals that the cell cycle is inhibited. F, Flow cytometry demonstrates that cell apoptosis is elevated. *$p<0.05$.

swell assay results showed that the knockdown of circ100284 and knockdown of PTEN or EMP1 reversed the decrease in cell migration and invasion caused by simple knockdown of circ100284 (Figure 5H). These data indicate that PTEN and EMP1 were lowly-expressed in OS tissues, and that circ100284 can negatively regulate the expression of PTEN or EMP1.

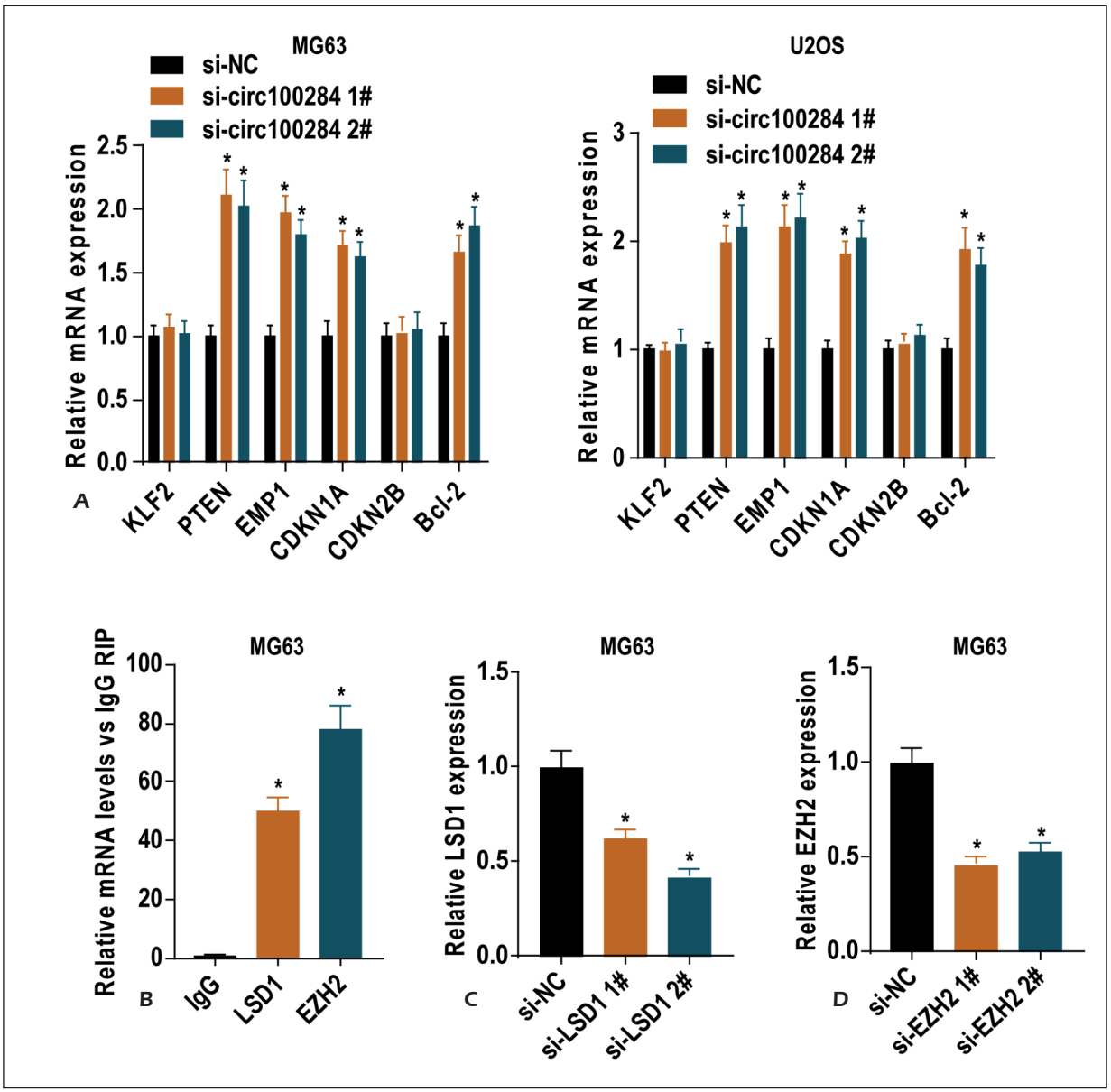

Figure 3. PTEN and EMP1 are regulated by circ100284. **A**, After knocking down circ100284 in MG63 and U2OS cells, mRNA expression levels of KLF2, PTEN, EMP1, CDKN1A, CDKN2B, and Bcl-2 are detected by qRT-PCR. **B**, In MG63 cells, RNA co-immunoprecipitation assay is used to detect the binding of CIRC100284 to LSD1 and EZH2 proteins. **C**, In MG63 cells, after LSD1 is knocked down, qRT-PCR reveals that the expression of LSD1 is significantly decreased. **D**, In MG63 cells, the expression of EZH2 is significantly decreased after knocking down EZH2.

Discussion

Osteosarcoma is the most common bone malignancy, with a high incidence in children and adolescents and a poor prognosis[24]. Therefore, finding the ideal biomarkers and therapeutic targets is of great significance for improving the diagnosis and treatment of OS.

CircRNAs are conserved and stable blocking RNA molecules that regulate cell proliferation and metastasis and plays an important role in tumorigenesis and development[25,26]. The circRNA circMAN2B2 promotes the proliferation and invasion of lung cancer cells through miR-1275[27]. Silencing of circRNA circ0000977 upregulates miR-871-3p expression and inhibits Polo-like kinase expression, thereby inhibiting the progression of pancreatic ductal adenocarcinoma[28]. A variety of circRNAs can promote the progression of OS, such as circ-NASP[29], circ-NT5C2[30], and circ0001562[31].

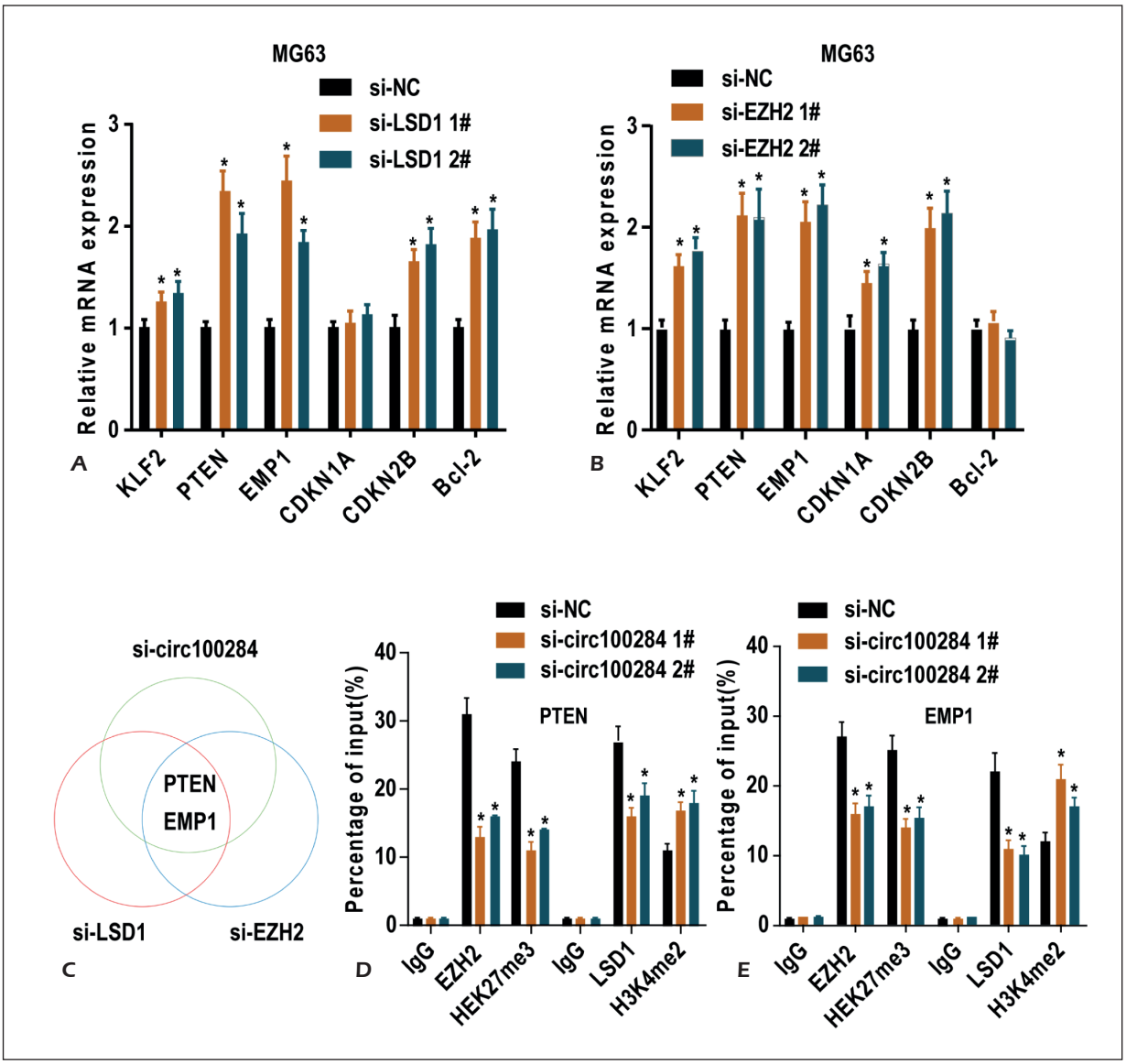

Figure 4. Circ100284 apparently silences PTEN and EMP1 by binding to LSD1 and EZH2. **A**, In MG63 cells, mRNA expression levels of KLF2, PTEN, EMP1, CDKN1A, CDKN2B, and Bcl-2 are detected by qRT-PCR after knockdown of LSD1. **B**, mRNA expression levels of KLF2, PTEN, EMP1, CDKN1A, CDKN2B, and Bcl-2 are measured by qRT-PCR after knockdown of EZH2 in MG63 cells. **C**, After knocking out circ100284, LSD1, and EZH2, the results of the co-variation of the genes show that only PTEM and EMP1 sustains an increased trend. **D**, Circ100284 is knocked out in MG63 cells, and ChIP-qPCR assay is used to determine the binding of LSD1, H3K27me3, and EZH2 to the PTEN promoter region. **E**, Circ100284 is knocked out in MG63 cells, and ChIP-qPCR assay is used to detect the binding of LSD1, H3K27me3, and EZH2 to the EMP1 promoter region. *p<0.05.

Few reports have been reported on the relationship between OS and circ100284 expression. In this study, it was found that circ100284 was highly expressed in OS, and the expression level of circ100284 was positively correlated with tumor size, stage and distant metastasis of OS and negatively correlated with patient survival rate. Cell experiments showed that knocking down circ100284 inhibited the viability, migration, and invasion of OS cells, leading to cell cycle arrest in GO/G1 phase and promoting OS cell apoptosis. Thus, circ100284 may play a role in cancer-promoting genes in OS.

There is evidence that circRNA regulates the expression of target genes by different mechanisms through different tumor cells. In this study, RNA immunoprecipitation assay was performed in MG-63 cells to find that circ100284 could directly bind to LSD1 and EZH2 proteins. LSD1 is a member of the nuclear histone demethylase[32] and

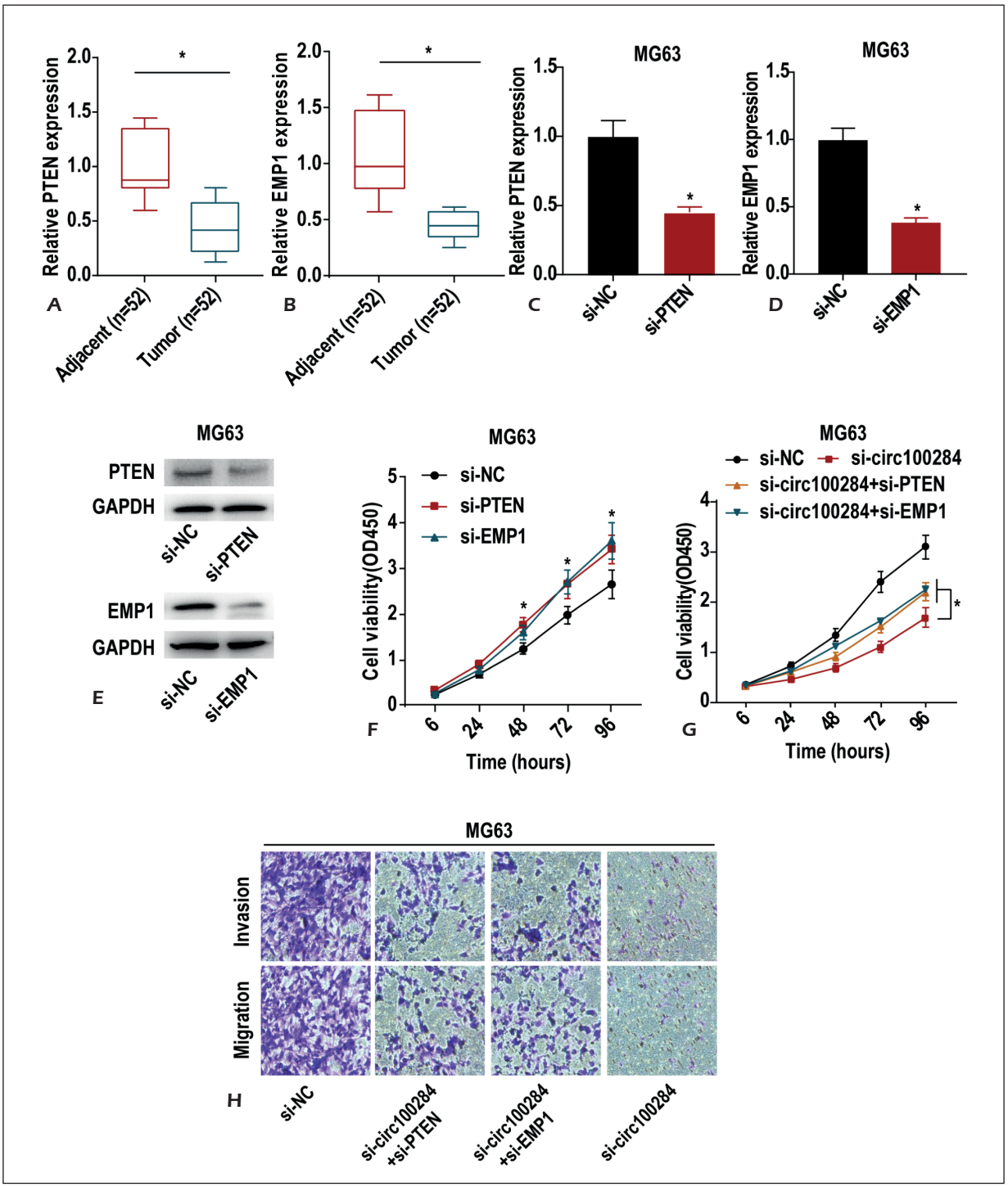

Figure 5. Circ100284 negatively regulates the expression of PTEN and EMP1. **A**, qRT-PCR verifies that PTEN expression in OS tissue is significantly lower than that in adjacent tissues. **B**, qRT-PCR manifests that EMP1 expression in OS tissues is significantly lower than that in adjacent tissues. **C**, PTEN is knocked down in MG63 cells, and the expression of PTEN is significantly decreased. **D**, EMP1 is knocked down in MG63 cells, and the expression of EMP1 is significantly decreased. E, Western blotting analysis shows that the protein expression level of PTEN is decreased after knockdown of PTEN in MG63 cells. After knockdown of EMP1, the protein expression level of EMP1 is decreased. **F**, After knocking down PTEN or EMP1 in MG63 cells, the viability of the cells is enhanced. **G**, In MG63 cells, knockdown of circ100284 and PTEN or EMP1 reverses the reduction of cell viability caused by simple knockdown of circ100284. **H**, In MG63 cells, simultaneous knockdown of circ100284 and PTEN or EMP1 reverses the effect of knockdown of circ100284 alone on cell migration and invasion (magnification: 40×). *p<0.05.

can regulate the balance between active chromatin, heterochromatin, and inhibition of chromatin[33,34]. EZH2 belongs to the multi-comb gene family and is highly conserved. It can inhibit the transcription of its downstream target genes, regulate the self-renewal of stem cells, and participate in embryonic development and tumorigenesis[35]. EZH2 protein is upregulated in a variety of tumors, and high expression of EZH2 may result in poor prognosis[36].

The PTEN was the first tumor suppressor gene discovered in 1997[37]. It has been reported that in bladder cancer cells, overexpression of PTEN inhibits the growth of bladder cancer cells and induces apoptosis by inhibiting the expression of surviving genes[38]. Overexpression of PTEN also induced growth arrest and apoptosis in human breast cancer ZR-75-1 cells[39] and human ovarian cancer cells[40]. Similarly, studies[41] have found that EMP1 is associated with a variety of tumors and can be used as a novel therapeutic target for human cancers. In the present study, PTEN and EMP1 were lowly expressed in OS. After knocking down PTEN or EMP1, cell viability was reduced and cell migration and invasion abilities were reduced. The results of cell recovery experiments revealed that simultaneous knockdown of circ100284 and PTEN or EMP1 reversed the decrease in cell viability, migration, and invasion ability caused by simple knockdown of circ100284. Thus, circ100284 can negatively regulate the expression of PTEN and EMP1 to exert its biological functions.

Conclusions

In summary, circ100284 is highly expressed in OS and can promote the proliferation, migration, and invasion of OS cells by apparently silencing the expression of PTEN and EMP1.

Conflict of Interests

The authors declare that they have no conflict of interest.

References

1) Lindsey BA, Markel JE, Kleinerman ES. Osteosarcoma overview. Rheumatol Ther 2017; 4: 25-43.
2) Biazzo A, De Paolis M. Multidisciplinary approach to osteosarcoma. Acta Orthop Belg 2016; 82: 690-698.
3) Yang Y, Han L, He Z, Li X, Yang S, Yang J, Zhang Y, Li D, Yang Y, Yang Z. Advances in limb salvage treatment of osteosarcoma. J Bone Oncol 2018; 10: 36-40.
4) Bielack SS, Hecker-Nolting S, Blattmann C, Kager L. Advances in the management of osteosarcoma. F1000Res 2016; 5: 2767.
5) Chen LL, Yang L. Regulation of circRNA biogenesis. RNA Biol 2015; 12: 381-388.
6) Sanger HL, Klotz G, Riesner D, Gross HJ, Kleinschmidt AK. Viroids are single-stranded covalently closed circular RNA molecules existing as highly base-paired rod-like structures. Proc Natl Acad Sci U S A 1976; 73: 3852-3856.
7) Hsu MT, Coca-Prados M. Electron microscopic evidence for the circular form of RNA in the cytoplasm of eukaryotic cells. Nature 1979; 280: 339-340.
8) Arnberg AC, Van Ommen GJ, Grivell LA, Van Bruggen EF, Borst P. Some yeast mitochondrial RNAs are circular. Cell 1980; 19: 313-319.
9) Kos A, Dijkema R, Arnberg AC, van der Meide PH, Schellekens H. The hepatitis delta (delta) virus possesses a circular RNA. Nature 1986; 323: 558-560.
10) Nigro JM, Cho KR, Fearon ER, Kern SE, Ruppert JM, Oliner JD, Kinzler KW, Vogelstein B. Scrambled exons. Cell 1991; 64: 607-613.
11) Capel B, Swain A, Nicolis S, Hacker A, Walter M, Koopman P, Goodfellow P, Lovell-Badge R. Circular transcripts of the testis-determining gene Sry in adult mouse testis. Cell 1993; 73: 1019-1030.
12) Zaphiropoulos PG. Circular RNAs from transcripts of the rat cytochrome P450 2C24 gene: correlation with exon skipping. Proc Natl Acad Sci U S A 1996; 93: 6536-6541.
13) Pasman Z, Been MD, Garcia-Blanco MA. Exon circularization in mammalian nuclear extracts. RNA 1996; 2: 603-610.
14) Salzman J, Chen RE, Olsen MN, Wang PL, Brown PO. Cell-type specific features of circular RNA expression. PLoS Genet 2013; 9: e1003777.
15) Jeck WR, Sorrentino JA, Wang K, Slevin MK, Burd CE, Liu J, Marzluff WF, Sharpless NE. Circular RNAs are abundant, conserved, and associated with ALU repeats. RNA 2013; 19: 141-157.
16) Memczak S, Jens M, Elefsinioti A, Torti F, Krueger J, Rybak A, Maier L, Mackowiak SD, Gregersen LH, Munschauer M, Loewer A, Ziebold U, Landthaler M, Kocks C, le Noble F, Rajewsky N. Circular RNAs are a large class of animal RNAs with regulatory potency. Nature 2013; 495: 333-338.
17) Hansen TB, Jensen TI, Clausen BH, Bramsen JB, Finsen B, Damgaard CK, Kjems J. Natural RNA circles function as efficient microRNA sponges. Nature 2013; 495: 384-388.
18) Zhang Y, Zhang XO, Chen T, Xiang JF, Yin QF, Xing YH, Zhu S, Yang L, Chen LL. Circular intronic long noncoding RNAs. Mol Cell 2013; 51: 792-806.
19) Li Z, Huang C, Bao C, Chen L, Lin M, Wang X, Zhong G, Yu B, Hu W, Dai L, Zhu P, Chang Z, Wu Q, Zhao Y, Jia Y, Xu P, Liu H, Shan G. Exon-intron circular RNAs regulate transcription in the nucleus. Nat Struct Mol Biol 2015; 22: 256-264.

20) Li F, Zhang L, Li W, Deng J, Zheng J, An M, Lu J, Zhou Y. Circular RNA ITCH has inhibitory effect on ESCC by suppressing the Wnt/beta-catenin pathway. Oncotarget 2015; 6: 6001-6013.

21) Bachmayr-Heyda A, Reiner AT, Auer K, Sukhbaatar N, Aust S, Bachleitner-Hofmann T, Mesteri I, Grunt TW, Zeillinger R, Pils D. Correlation of circular RNA abundance with proliferation--exemplified with colorectal and ovarian cancer, idiopathic lung fibrosis, and normal human tissues. Sci Rep 2015; 5: 8057.

22) Xue J, Liu Y, Luo F, Lu X, Xu H, Liu X, Lu L, Yang Q, Chen C, Fan W, Liu Q. Circ100284, via miR-217 regulation of EZH2, is involved in the arsenite-accelerated cell cycle of human keratinocytes in carcinogenesis. Biochim Biophys Acta Mol Basis Dis 2017; 1863: 753-763.

23) Dai X, Chen C, Yang Q, Xue J, Chen X, Sun B, Luo F, Liu X, Xiao T, Xu H, Sun Q, Zhang A, Liu Q. Exosomal circRNA_100284 from arsenite-transformed cells, via microRNA-217 regulation of EZH2, is involved in the malignant transformation of human hepatic cells by accelerating the cell cycle and promoting cell proliferation. Cell Death Dis 2018; 9: 454.

24) Ottaviani G, Jaffe N. The epidemiology of osteosarcoma. Cancer Treat Res 2009; 152: 3-13.

25) Jeck WR, Sharpless NE. Detecting and characterizing circular RNAs. Nat Biotechnol 2014; 32: 453-461.

26) Zeng K, Chen X, Xu M, Liu X, Hu X, Xu T, Sun H, Pan Y, He B, Wang S. CircHIPK3 promotes colorectal cancer growth and metastasis by sponging miR-7. Cell Death Dis 2018; 9: 417.

27) Ma X, Yang X, Bao W, Li S, Liang S, Sun Y, Zhao Y, Wang J, Zhao C. Circular RNA circMAN2B2 facilitates lung cancer cell proliferation and invasion via miR-1275/FOXK1 axis. Biochem Biophys Res Commun 2018; 498: 1009-1015.

28) Huang WJ, Wang Y, Liu S, Yang J, Guo SX, Wang L, Wang H, Fan YF. Silencing circular RNA hsa_circ_0000977 suppresses pancreatic ductal adenocarcinoma progression by stimulating miR-874-3p and inhibiting PLK1 expression. Cancer Lett 2018; 422: 70-80.

29) Huang L, Chen M, Pan J, Yu W. Circular RNA circNASP modulates the malignant behaviors in osteosarcoma via miR-1253/FOXF1 pathway. Biochem Biophys Res Commun 2018; 500: 511-517.

30) Liu X, Zhong Y, Li J, Shan A. Circular RNA circNT5C2 acts as an oncogene in osteosarcoma proliferation and metastasis through targeting miR-448. Oncotarget 2017; 8: 114829-114838.

31) Song YZ, Li JF. Circular RNA hsa_circ_0001564 regulates osteosarcoma proliferation and apoptosis by acting miRNA sponge. Biochem Biophys Res Commun 2018; 495: 2369-2375.

32) Hoffmann I, Roatsch M, Schmitt ML, Carlino L, Pippel M, Sippl W, Jung M. The role of histone demethylases in cancer therapy. Mol Oncol 2012; 6: 683-703.

33) Goldberg AD, Allis CD, Bernstein E. Epigenetics: a landscape takes shape. Cell 2007; 128: 635-638.

34) Albert M, Peters AH. Genetic and epigenetic control of early mouse development. Curr Opin Genet Dev 2009; 19: 113-121.

35) Schramek D, Sendoel A, Segal JP, Beronja S, Heller E, Oristian D, Reva B, Fuchs E. Direct in vivo RNAi screen unveils myosin IIa as a tumor suppressor of squamous cell carcinomas. Science 2014; 343: 309-313.

36) Ha SY, Kim SH. Co-expression of Bmi1 and EZH2 as an independent poor prognostic factor in esophageal squamous cell carcinoma. Pathol Res Pract 2012; 208: 462-469.

37) Li J, Yen C, Liaw D, Podsypanina K, Bose S, Wang SI, Puc J, Miliaresis C, Rodgers L, McCombie R, Bigner SH, Giovanella BC, Ittmann M, Tycko B, Hibshoosh H, Wigler MH, Parsons R. PTEN, a putative protein tyrosine phosphatase gene mutated in human brain, breast, and prostate cancer. Science 1997; 275: 1943-1947.

38) Wu ZX, Song TB, Li DM, Zhang XT, Wu XL. Overexpression of PTEN suppresses growth and induces apoptosis by inhibiting the expression of survivin in bladder cancer cells. Tumour Biol 2007; 28: 9-15.

39) Li X, Lin G, Wu B, Zhou X, Zhou K. Overexpression of PTEN induces cell growth arrest and apoptosis in human breast cancer ZR-75-1 cells. Acta Biochim Biophys Sin (Shanghai) 2007; 39: 745-750.

40) Yan X, Fraser M, Qiu Q, Tsang BK. Over-expression of PTEN sensitizes human ovarian cancer cells to cisplatin-induced apoptosis in a p53-dependent manner. Gynecol Oncol 2006; 102: 348-355.

41) Wang YW, Cheng HL, Ding YR, Chou LH, Chow NH. EMP1, EMP 2, and EMP3 as novel therapeutic targets in human cancer. Biochim Biophys Acta Rev Cancer 2017; 1868: 199-211.